Electrical Impedance Characterization of Bone Fractures in Presence of an Intramedullary Nail

Li, Yunfeng; Mikkelsen, Jan H.; Zhekov, Stanislav Stefanov; Jensen, Ole Kiel; Frost, Markus Winther; Kold, Søren Vedding; Pedersen, Gert Frølund; Shen, Ming

Published in:
The 20th IEEE International Conference on BioInformatics And BioEngineering

DOI (link to publication from Publisher):
10.1109/BIBE50027.2020.00119

Publication date:
2020

Document Version
Early version, also known as pre-print

Electrical Impedance Characterization of Bone Fractures in Presence of an Intramedullary Nail

Yunfeng Li[#1], Jan H. Mikkelsen[#2], Stanislav S. Zhekov[#3], Ole K. Jensen[#4], Markus W. Frost[*5], Søren Kold[*6], Gert F. Pedersen[#7], Ming Shen[#8]

[#]Department of Electronic Systems, Aalborg University, Denmark
[*]Department of Orthopedics, Aalborg University Hospital, Denmark
{[1]yli, [2]jhm, [3]stz, [4]okj, [7]gfp, [8]mish}@es.aau.dk, {[5]markus.frost,[6]sovk}@rn.dk

***Abstract*— This paper presents an electrical impedance characterization and measurement method for monitoring bone fracture healing progress after osteosynthesis, for cases applying an intramedullary nail. While existing solutions fail due to the presence of the nail, the proposed method makes active use of the nail to achieve accurate healing progress monitoring. The proposed method captures variations in the electrical impedance at the fracture site as body tissues transform from blood (hematoma) to fully recovered intact bone during healing. The proposed method therefore has the potential to be used for data acquisition of bone healing and pave the way for digitized diagnosis and treatment of bone fractures.**

***Keywords*— bone healing, electrical impedance spectroscopy, intramedullary nail.**

I. Introduction

Each year many people suffer the experience of bone fracture. In the US alone, an estimated 12 - 15 million bone fractures are treated on a yearly basis [1]. Depending on the nature of the fracture, patients may - in best cases - receive a simple plaster cast. However, in the case of non-union fractures, where natural healing is not possible and surgical intervention is needed, the process can be long and painful.

Non-union represents a serious complication in fracture healing and it can result from several reasons. The most typical ones are excessive fracture movement during the healing process, poor blood supply to the fracture gap region or infections. Targeting the former, immobilization of the fracture is a well-known remedy that has been used for decades. Here, use of a plaster cast typically has to be supplemented by prolonged periods of patient inactivity to ensure healing. Another approach is to achieve stabilization using in-vivo metal plates, pins, screws or rods. Here, the intramedullary nail (IM nail), which is a metal rod inserted into the medullary cavity of the fractured bone, as shown in Fig. 1 (c), has been demonstrated leading to much faster return to activity [2].

To continuously asses the post-operative healing state of a complex fracture the typical clinical routine is to make use of radiography. By regularly comparing images, potential healing progress in the fracture may be observed. However, not only does this practice lead to excessive exposure to ionizing radiation, the information provided by radiography is also highly dependant on the experience of the medical staff and - more importantly - it does not, directly, provide details of the bio-mechanical properties of the fracture site it self [3], [4]. A means to accurately asses the mechanical properties of the fracture without the need for radiography is therefore highly desired.

When an implant is first used the majority of the load is on the implant itself. Over time, as the fractured bone heals and regenerates, the bone gradually begins to absorb more and more of the load. Measuring the resulting load on the implant therefore provides an indication of the mechanical state of the healing fracture. Over time, a number of monitoring techniques have been developed to asses the mechanical properties of various implant systems [5]. The typical approach is to apply some form of strain gauge to monitor the load forces imposed on the implant. More recently, electrical impedance spectroscopy (EIS) measurements have been pursued to obtain insight into fracture properties [6], [7]. Here, differences in electrical characteristics of different tissues are exploited to provide a measure of the tissue composition within the fracture region. As shown in Fig. 1 reported EIS approaches are limited to longitudinal impedance measurements only (Fig. 1 (a)) [6], or, in addition, to overcome noise from surrounding tissue, measurement electrodes have to be placed directly in the fracture gap (Fig. 1 (b)) [7]. Also, external structures are generally used to stabilize sensor positions and it is unclear how to remove the need for such ex-vivo structures. For fracture cases where IM nails are inserted, existing EIS methods generally fail as the nail it self provides a low impedance current path, which interferes with the measurements. As such, impedance measurements are generally unsuited for load measurements on fractures treated with IM nails.

In this paper an EIS-based approach capable of overcoming this limitation is proposed. The proposed method, which is illustrated in Fig. 1 (c), is novel in that the IM nail it self is used as an active element in the measurement system. Furthermore, the proposed method does not add extra electrodes to the fracture gap it self, thereby providing less interference directly to the fracture callus. Finally, the required electrical setup is compact and easily implantable, whereby the whole healing process can be monitored without the need for skin protruding wires or metal rods.

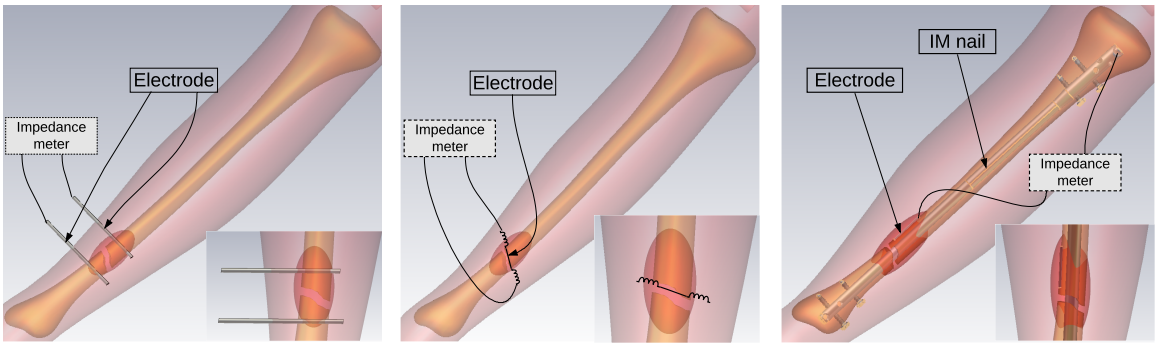

(a) (b) (c)

Fig. 1. Illustrations of existing EIS methods where (a) the electrodes are transversally penetrating the bone [6], or (b) directly passing through the fracture gap [7], and (c) the proposed technique which utilizes the IM nail and an electrode to measure the transversal electrical impedance of the tissue at the fracture gap.

II. Theoretical Analysis

The physical structure of a fracture area is very complex and hence difficult to model accurately. For a feasible mathematical analysis of the correlation between fracture healing and electrical impedance, a simplified cylindrical model, as illustrated in Fig. 2, is adopted here.

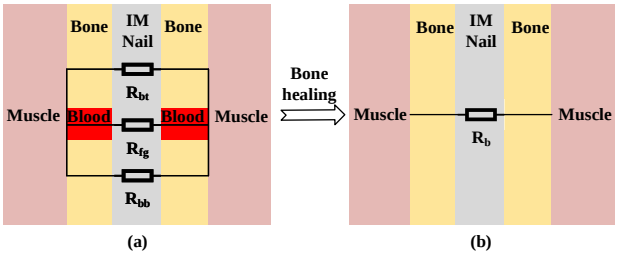

Fig. 2. Side-view illustration of the proposed electrical impedance model where (a) shows the impedance model for a fractured bone, while (b) shows the model for a healed bone.

The different layers of the model represent the various tissue materials found at the fracture site. Innermost is the intramedullary nail, which is surrounded by the actual bone structure, which again is surrounded by soft tissue, such as muscle. When a fracture occurs the continuity of the bone is broken and the gap is initially filled by a haematoma (blood). The electrical impedance models illustrated in Figs. 2a and 2b use R_{fg} to represent the resistance of the fracture gap, while R_{bt} and R_{bl} represent the bone resistance above and below the fracture gap respectively. For a fully healed fracture the resulting resistance is represented by R_b.

As the conductivity of blood is significantly higher than that of bone, as shown in Table 1, the electrical characteristics of the two cases illustrated in Fig. 2 are quite different. For the fracture case, the majority of the current therefore flows through the fracture tissue resulting in a much lower electrical impedance than what would result for a healed bone fracture.

For a simple cylindrical shape the transversal resistance, R_c, from the center and out can be expressed as

$$dR_c = dr \cdot \frac{1}{\delta} \cdot \frac{1}{2\pi r L}, \tag{1}$$

Table 1. Electrical properties for body tissues measured at 100 Hz [8].

Tissue type	Permittivity [F/m]	Conductivity [S/m]
Bone marrow	85000	0.003
Bone cortical	3000	0.02
Cartilage	-	0.18
Blood	3000 (@ 1 kHz)	0.7
Muscle	$1 * 10^7$	0.35

where δ is the conductivity, r is the radius of the cylinder and L is the length of the cylinder.

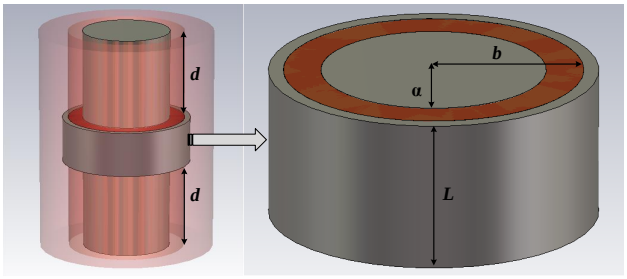

Fig. 3. Simplified physical structure for resistance calculation and simulations.

For a hollow cylindrical shape, as illustrated in Fig. 3, Eq. (1) takes the form of

$$R_c = \int_a^b dR = \frac{1}{2\pi L\delta}\int_a^b \frac{1}{r}dr = \frac{1}{2\pi L\delta}\ln\frac{b}{a}, \tag{2}$$

where a and b are the inner and outer radii of the shape respectively. For the length of the electrode, the resulting total resistance is the parallel connection of the three components R_{fg}, R_{bt} and R_{bl}, as illustrated in Fig. 2a. As the bone fracture heals the total resistance should equal R_{fg} at first and eventually converge towards R_b as bone cortical forms.

To evaluate the theory, 3D simulations of the simplified model are carried out using CST and compared to results based on Eq. (2). Moreover, simulations are carried out using the setup in Fig. 2, where a bone length of 80 mm, a fracture gap, L, varied from 1 mm to 40 mm, and a bone diameter of 20 mm is used. From the simulation results shown in Fig. 4, the correlation between transversal impedance and

tissue conductivity is evident. Also, the results show very good agreement between the simple impedance model and simulations.

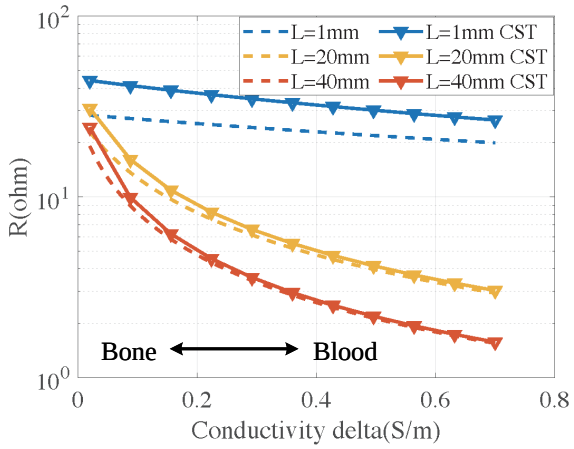

Fig. 4. Calculated and simulated impedance values versus tissue conductivity for different sized fracture gaps. The results assume 40 mm bone length above and below the fracture gap and diameters of 20 mm and 15 mm for the bone and the IM nail respectively. Dashed lines represent theoretical analysis values.

III. Simulations

To demonstrate the capabilities and the feasibility of the proposed method a number of full-3D simulations are conducted using CST based on the lower leg model illustrated in Fig. 1. In the simulation, the outer electrode is 30 mm in length and 4 mm in diameter with a distance of 5 mm to the top edge of the fracture.

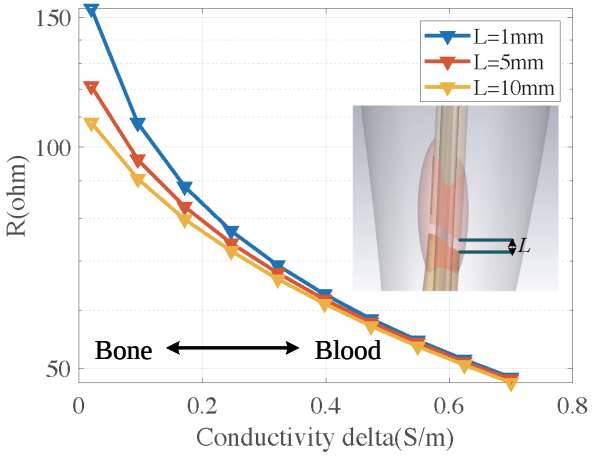

Fig. 5. Simulated impedance values for the setup in Fig. 1 for different fracture gap settings. The electrode is 30 mm in length and 4 mm in diameter. The distance between electrode and gap is 5 mm.

Fig. 5 shows that the electrical impedance between the IM nail and the outer electrode increases more than two times as the fracture tissue transforms from blood to bone. Dimensions of the electrode are kept constant for all three values of L, which is why the impedance values are quite similar. However, this does not interfere with the objective, which is to capture impedance variation due to fracture tissue transformation.

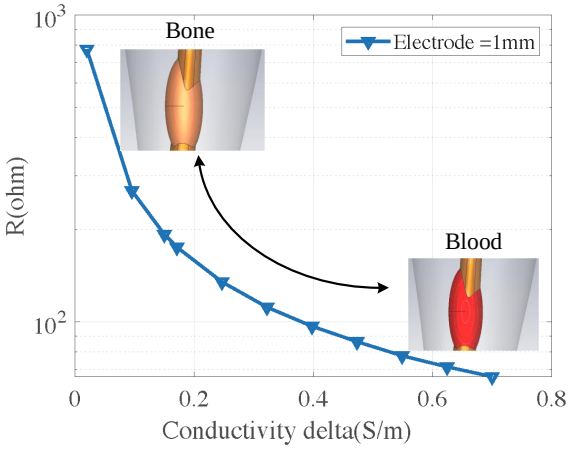

Fig. 6. Simulated electrical impedance value at the fracture site when the diameter of the outer electrode is 1 mm.

It should be noted that reducing the diameter of the outer electrode increases the impedance difference between the two case, that is i) a new fracture filled with blood and ii) a healed bone. This is illustrated in Fig. 6 for an outer electrode diameter of 1 mm. The significant difference in impedance values between the two cases can also be explained by the current density at the bone fracture site, as shown in Fig. 7. When the gap is filled with haematoma (Fig. 7d) at an early stage of bone healing the major part of the current flows through the haematoma, resulting in a low impedance value. In contrast, at a later stage of bone healing, the current flows more uniformly between the IM nail and the outer electrode, leading to a higher impedance value (Fig. 7a).

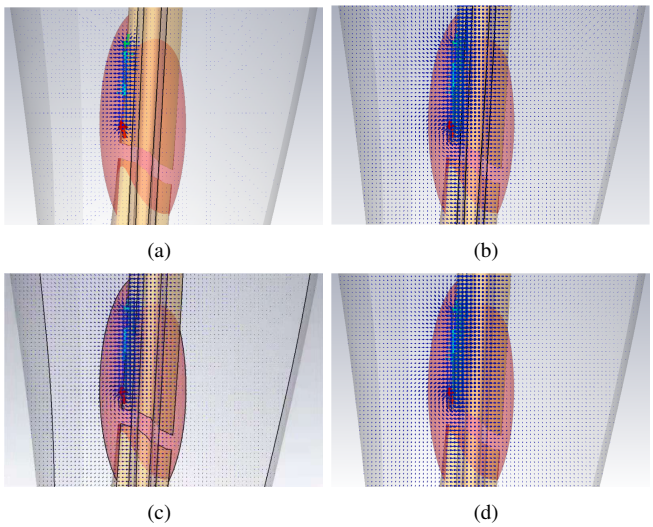

Fig. 7. Simulated current density at the fracture site when (a) delta = 0.02 S/m, (b) delta = 0.15 S/m, (c) delta = 0.36 S/m, and (d) delta = 0.7 S/m.

IV. Experimental Validation

In-vitro measurements have been carried out with rabbit tibias to validate the proposed impedance model and measurement approach. An IM nail consisting of a 7.5 cm

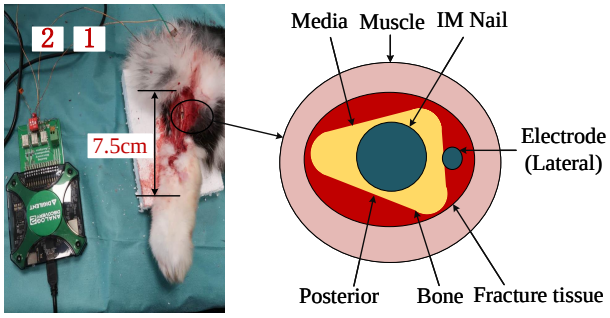

Fig. 8. Rabbit tibia in vitro experimental setup (left) and the location of the IM nail and electrode (right).

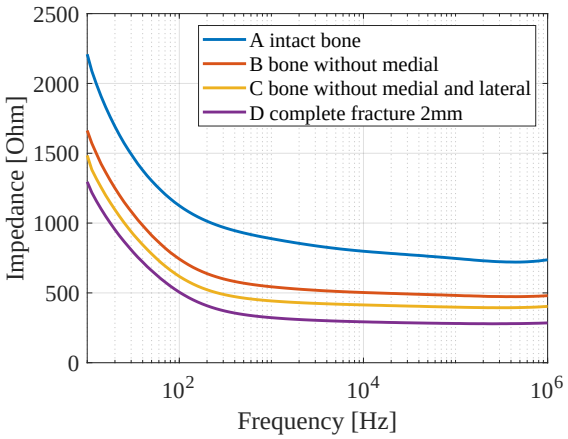

Fig. 9. Measured impedance for different cases that emulates the reverse process of bone healing.

long brass wire with a diameter of 1.5 mm was used in the experiment. The locations of the IM nail and the electrode are as shown in Fig. 8. The distance from the electrode to the fracture gap was 5mm for all tests. The impedance between the IM nail and the electrode was measured across a frequency band from 10 Hz to 1 MHz.

In the experiment the different sides of the rabbit tibia (Media, Lateral, and Posterior in Fig. 8) were removed to emulate different fracture tissue compositions during bone healing. The cases tested include complete fracture with 2 mm fracture length (case D), bone without medial and lateral (case C), bone without medial (case B), and intact bone (case A). The measured impedance for each case are shown in Fig. 9.

From Fig. 9 it is clear that different tissue composition cases can be easily distinguished from each other based on the differences between impedance curves. The impedance for the complete fracture case, with three different fracture gap lengths, are also measured and results are shown in Fig. 10. As can be seen the impedance values for the three cases are quite similar. This is because the same outer electrode was used for all the tests. All measurement results are consistent with the theoretical analysis and simulation.

V. Conclusion

In this paper a method for characterization of bone fracture healing in presence of an intramedullary (IM) nail is proposed.

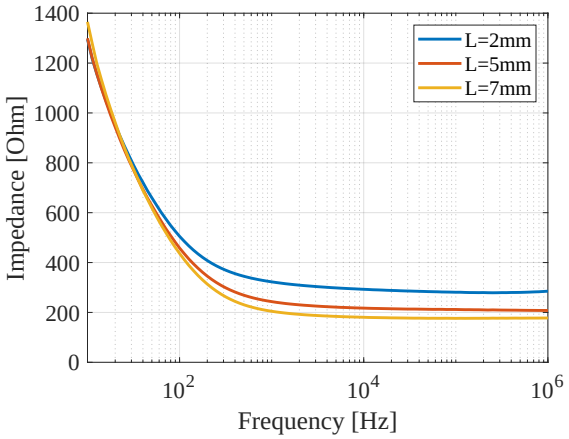

Fig. 10. Measured impedance for different fracture gap lengths.

The method is based on the principle of electrical impedance spectroscopy and is novel in that it makes active use of the IM nail, while conventional EIS methods all fail when a fracture is stabilized using an IM nail. A theoretical framework is presented and used to show a clear correlation between impedance values and bone regeneration. Using a simplified 3D simulation structure the theoretical framework is validated and proven to match very accurately with simulation results. Extensive full-3D simulations of a human tibia with an IM nail inserted are used to demonstrate the feasibility of the method. Finally, measurement results based on a rabbit bone are provided and good agreement between simulations and measurements are observed.

Acknowledgment

The authors would like to acknowledge the support of Ben K. Krøyer throughout this work.

References

[1] A. Pollak and S. Watkins-Castillo, "The bone and joint initiative. fracture trends. the burden of musculoskeletal diseases in the united states," *Available at www.boneandjointburden.org/2014-report/via23/fracture-trends. (Accessed: 11th February 2020).*

[2] G. Hooper, R. Keddell, and I. Penny, "Conservative management or closed nailing for tibial shaft fractures. a randomised prospective trial," *Bone Joint Surg Br.*, vol. 73, no. 1, pp. 83–85, 1991.

[3] M. Faschingbauer and K. Seide, "Das intelligente implantat," *Trauma und Berufskrankheit*, vol. 11, no. 1 - suppl, pp. 60–64, 2009.

[4] T. Blokhuis, J. de Bruine, J. Bramer, F. den Boer, F. Bakker, P. Patka, H. Haarman, and R. Manoliu, "The reliability of plain radiography in experimental fracture healing," *Skeletal Radiology*, vol. 30, no. 3, pp. 151–156, 2001.

[5] L. Claes and J. Cunningham, "Monitoring the mechanical properties of healing bone," *Clinical Orthopaedics and Related Research*, vol. 467, no. 8, pp. 1964–1971, 2009.

[6] M. Lin, F. Yand, S. Herfat, C. Bahney, M. Marmor, and M. Maharbiz, "New opportunities for fracture healing detection: Impedance spectroscopy measurements correlate to tissue composition in fractures," *Orthopaedic Research*, vol. 35, no. 12, pp. 2620–2629, 2017.

[7] M. Lin, D. Hu, M. Marmor, S. Herfat, C. Bahney, and M. Maharbiz, "Smart bone plates can monitor fracture healing," *Scientific Reports*, vol. 9, p. 2122, 2019.

[8] C. Gabriel, “Compilation of the dielectric properties of body tissues at rf and microwave frequencies.” *U.S. Air Force Report AFOSR-TR-96*, 1996.